Evaluation of Rock/Fracture Interactions During Steam Injection Through Vertical Hydraulic Fractures

A.R. Kovscek, SPE, Stanford U., **R.M. Johnston,** SPE, CalResources LLC, and **T.W. Patzek,** SPE, U. of California at Berkeley

Summary

The design, results, and analysis of a steamdrive pilot in the South Belridge diatomite, Kern County, California, are reviewed. Pilot results demonstrate that steam can be injected across a 1,000-ft-tall diatomite column using hydraulically fractured wells and that significant oil is produced in response to steaming. A computationally simple numerical model is proposed and used to analyze reservoir heating and volumetric sweep by steam. Results from the analysis show that hydraulic fractures undergoing steam injection can be dynamic and asymmetrical.

Introduction

Estimates of the original oil in place (OOIP) for the diatomaceous oil fields of California, located in the southern San Joaquin Valley near Bakersfield, exceed 10 billion bbl.[1] This exceptionally large OOIP, combined with the fact that these fields are onshore and relatively well characterized, makes them an attractive target for production.

However, relatively low rock permeability (0.01 to 10 md), the highly layered nature of the diatomite, and the tendency of diatomaceous rocks to fracture conspire against production.[2] To date, most production from the diatomite has occurred under either primary or waterflooding operations. In general, wells must be hydraulically fractured to improve production and offset low formation permeability. Waterflood operations on 1¼- and 5/8-acre spacing in light-oil diatomite have shown some success,[2,3] but also suffered from low injectivity, hence high wellhead pressures, and unwanted extension of hydraulically induced and natural fractures. In some cases, fracture extensions have led to injector/producer linkage.[2]

Steamdrive on 5/8-acre spacing is an attractive alternative. The primary advantage of steam over water injection is that through thermal conduction heat can sweep portions of the reservoir, steam does not enter directly. Oil recovery occurs through displacement of oil by steam and hot water, and also indirectly by volumetric expansion as oil warms.

Fig. 1 illustrates the possible benefits of steam injection and compares recovery with steamdrive to waterflood on 1¼- and 5/8-acre spacing. Recovery functions were computed by reservoir simulation with "typical" South Belridge diatomite properties, "typical" light-oil volumetric properties, formation layering, relative permeabilities, and capillary pressures. Cumulative oil recovery as the percentage of OOIP is presented vs. years of injection. The arrow at the lower left of the figure indicates that the recovery on primary is expected to be roughly 5% of the OOIP. Indefinite primary recovery is not possible because of formation compaction and reservoir subsidence. Most primary patterns in the diatomite were developed on 2½-acre spacing. Hence, many waterfloods were developed by drilling infill wells on 1¼-acre patterns. Fig. 1 predicts that even after 40 years of water injection, oil recovery on 1¼-acre spacing will be only 10% of the OOIP. Waterflood on 5/8-acre spacing is predicted to do better, with recovery at roughly 22% of the OOIP after 40 years. Neither of these predictions accounts for any formation damage that might limit oil recovery. In contrast to waterflood, steamdrive on 5/8-acre spacing is estimated to recover in excess of 40% of the OOIP after 40 years of injection. That is, twice as much oil as waterflood is recovered on the same spacing.

Although oil recovery from low-permeability, hydraulically fractured rock under steamdrive operations appears to possess great potential, there are many aspects of the technology left to understand. Further, the large density of wells associated with 5/8-acre spacing dictates that we move beyond rudimentary understanding. Some important aspects that need to be elucidated are the dynamics of hydraulically fractured wells undergoing steam injection, and how effectively such hydraulic fractures communicate heat and hot fluids to the formation. Steam is very compressible and condenses upon contacting cold portions of rock; thus, it is likely that lengthy transients in hydraulic-fracture performance occur.

A number of steam-injection projects in the diatomite have been or are being conducted to assess the viability of thermal recovery. These include a heavy-oil pilot in the Lost Hills diatomite operated by Mobil; a cyclic, heavy-oil injection project at Cymric carried out by Chevron[4]; and three separate light-oil pilots in the South Belridge diatomite conducted by Shell and later by CalResources.[5] These are denoted the Phase I, II, and III steamdrive projects. The second, or Phase II, steamdrive pilot uses two separate and noninteracting hydraulic fractures to inject steam across the entire diatomite column. Seven temperature-observation wells distributed across the pilot area allow monitoring of the progress of heat into the formation.

This paper presents a summary of the design and oil-recovery results from the Phase II pilot. We also present our efforts to interpret quantitatively formation response to steaming through both the upper and lower hydraulic fractures. Our goal is to understand both how quickly a hydraulic fracture fills with steam, and the interactions between a steam-filled fracture and the rock matrix.

Phase II Steamdrive Pilot

At South Belridge, the diatomite lies between depths of roughly 500 and 2,000 ft. Overlying the diatomite are the Tulare sands while the brown shale lies immediately below.

In the full-interval Phase II pilot conducted in Section 29, two injectors, referred to as IN2U and IN2L, were drilled close to each other and then hydraulic fractures were induced from 1,110 to 1,460 ft and from 1,560 to 1,910 ft, respectively. **Fig. 2** presents a plan view of the Phase II steam-injection pilot including injection, production, and monitoring wells. Note the scale of 100 ft in the lower right corner; well spacing is quite close. IN2U and IN2L are located in the center of Fig. 2 and are marked with darkened triangles. Separate injectors are advantageous as diatomite properties vary with depth and time. For instance, depending on depth and temperature, the unstable biogenic or inorganic silica of diatomite is found as Opal-A, which may dissolve and reprecipitate as metastable Opal-CT. Opal-CT in turn may dissolve and reprecipitate as microcrystalline quartz.[6]

A new producer, 543P, was drilled approximately 40 ft to the east of the injection wells and completed across the most permeable diatomite layers, 1,540 to 1,890 ft. The purpose of 543P was to quantify the early response of the diatomite to steam injection. Well 543N is an old, full-interval producer, drilled in October 1979, 130 ft to the west of the injection wells. By October 1989 it had produced 280,000 bbl of oil and 120,000 bbl of water. This well provided a cross reference for 543P and quantified the long-time response to steam injection. Both producers are marked with darkened circles on Fig. 2.

Original SPE manuscript received for review 11 April 1995. Paper peer approved 19 February 1997. Paper (SPE 29622) first presented at the 1995 SPE Western Regional Meeting held in Bakersfield, California, 8–10 March.

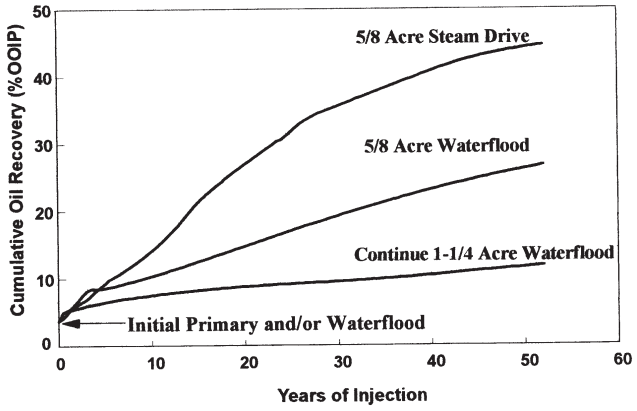

Fig. 1—Predicted recovery functions for diatomaceous formations.

Wells IN2U, IN2L, and 543P were imaged during the fracturing process, and thus the initial hydraulic-fracture shapes and orientations were fairly well characterized.[1,7] In short, the azimuth of hydraulic fractures in IN2U and IN2L is roughly N21°E with an error of about 4°. Both fractures were vertical, but the shapes were quite different. The IN2U fracture was asymmetrical, while the IN2L fracture was symmetrical. The dark diagonal lines in Fig. 2, passing through the injection and production wells, indicate hydraulic-fracture orientation with a N21°E azimuth. Microseismic monitoring showed that the hydraulic fracture in 543P was nearly vertical, divided in two separate zones corresponding to the most permeable diatomite layers, and the azimuth trended N25°E±5°.[7]

Several additional wells, LO11 to LO15 and MO2, were drilled and used to measure the formation-temperature response and oil displacement. The orientation of the observation wells relative to the injection hydraulic fractures allows monitoring of the areal extents of growth of steam zones as functions of depth and the growth of the cross-sectional area of the injection fractures. Further, neutron and gamma-ray spectroscopy tool (GST) logs were taken in LO11, L013 to LO15, and in 543N and 543P before steam injection.

Injection in IN2U began on 10 October 1990, while injection in IN2L followed 2 weeks later on 24 October 1990. Daily averages of the minute-by-minute measurements of steam-injection rate and pressure were saved for each injection well. Likewise, the production response was measured daily. Temperature surveys in the observations wells were run on average every 30 days between 800 and 2,000 ft at 10 ft intervals.

Phase II Response. Steam injectivity in both IN2U and IN2L was initially low, but increased over time. Tip extensions of the hydraulic fractures were mainly responsible for improvement in injection,

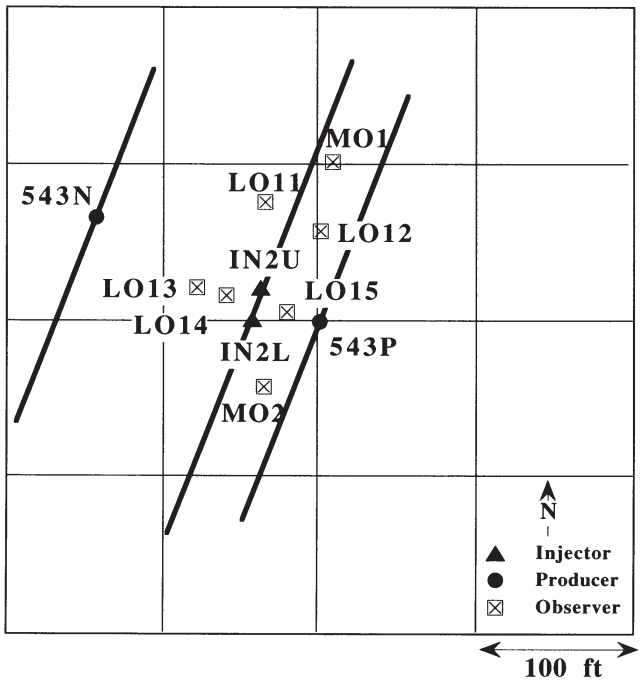

Fig. 2—Plan view of the Phase II steamdrive project.

with a secondary influence exerted by increasing injection pressure. IN2L experienced an overall 15-fold increase in injectivity and IN2U a 10-fold increase. **Figs. 3 and 4** show cumulative steam injection for IN2U and IN2L, respectively, in cold-water equivalents (CWE) as a thick dashed line versus the square root of time. The choice of square root of time as the natural time scale will become clear as the model equations are discussed. The increase in slope of these curves is indicative of increasing injectivity. These figures also show that cumulative steam injection reached 175,000 bbl CWE in IN2U and 214,000 bbl CWE in IN2L.

Interestingly, both producers show an oil response that correlates with steam injection. A massive horizontal opening and linking of natural fractures west of IN2U (as indicated by temperature surveys[8]) attracted by a low-pressure region extending all the way from the old producer 543N, resulted in a significant oil production response in 543N after 680 days of steam injection (**Fig. 5**). At the onset of the pilot, production averaged 40 BOPD while at the end it averaged 150 BOPD. A somewhat earlier response in Well 543P demonstrated strong linkage with the IN2L fracture (**Fig. 6**). A cocurrent water response was observed in 543N without heat or steam breakthrough, and in 543P with a dramatic steam breakthrough and a wellhead temperature reaching roughly 320°F. The cold producer

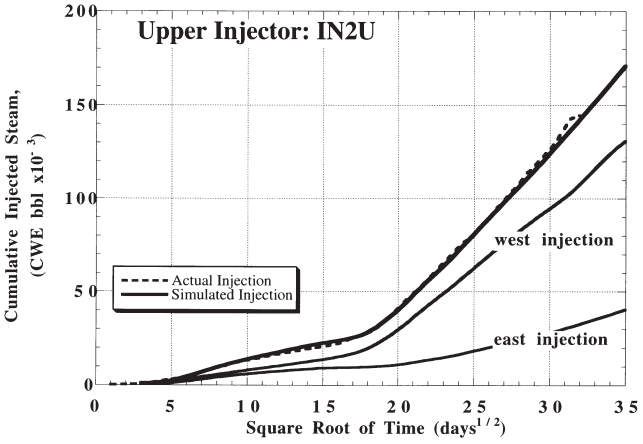

Fig. 3—Steam injection in IN2U, including injection to the east and west halves of the pilot.

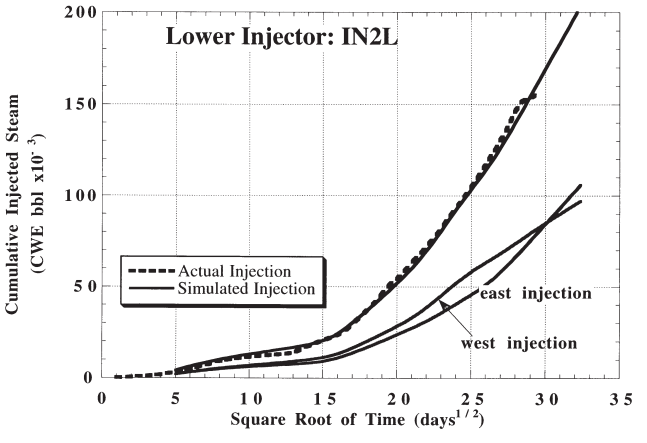

Fig. 4—Steam injection in IN2L, including injection to the east and west halves of the pilot.

543N appears to plug initially, as the second derivative of production with respect to the square root of time is −2,500 bbl/D. After 70 days$^{1/2}$ of steam injection, productivity turns from negative to positive and increases to +1,300 bbl/D. The productivity of 543P increases all of the time as the second derivative of production, just after steam breakthrough was about 400 bbl/D.

Figs. 5 and 6 show that cumulative oil production during the pilot (October 1990 to November 1995) was 106,000 bbl oil for 543N and 55,000 bbl oil for 543P. The incremental oil production above primary is estimated at 75,000 and 37,000 bbl oil for 543N and 543P, respectively.[9] Based upon estimation of both the pore and oil volumes in the pilot,[9] the cumulative recovery was calculated to be 9% of the OOIP, and the incremental recovery was 7% of the OOIP after 5 years of steam injection. The cumulative recovery compares favorably with the prediction in Fig. 1.

Model Description

Our computational approach is to lump the parameters which describe the first-order physics of steam movement in the diatomite into a single parameter, termed the hydraulic diffusivity, thereby simplifying history matching. This formulation leads to a second-order, partial-differential equation, similar in form to a transient diffusion equation, that describes the pressure profile in the steam-occupied zone of each layer of the diatomite.[9] The method of Marx and Langenheim[10] is then used to locate the steam front in each layer. Finally, the transient heat-conduction equation is solved for the temperature profile in the oil zone downstream of the steam front. The hydraulic and thermal diffusivities as well as the fracture shape are then iterated to match the areal temperature response in each layer of the diatomite in the Phase II pilot and the overall, cumulative steam injection.

Our approach is computationally efficient and leads to multiple realizations of steamdrive dynamics in the diatomite. More importantly, this modeling effort provides the precursory knowledge of fracture size and shape, as well as the relative changes in formation permeability needed to simulate steamdrive in the diatomite with fully compositional, multidimensional reservoir simulators.

The pressure-diffusion equation is derived by writing the usual continuum mass and energy balance equations for a black-oil reservoir simulation model and expanding spatial derivatives. Neglecting high-order derivative terms, gravity, capillarity, and assuming saturated-steam conditions[9] yields

$$\frac{\partial^2 p}{\partial x^2} = \frac{1}{\eta}\frac{\partial p}{\partial t}, \quad \ldots\ldots\ldots\ldots\ldots\ldots\ldots\ldots\ldots\ldots\ldots\ldots\ldots\ldots (1)$$

where the hydraulic diffusivity

$$\eta = \frac{\lambda_T}{c_T} \ldots\ldots\ldots\ldots\ldots\ldots\ldots\ldots\ldots\ldots\ldots\ldots\ldots\ldots\ldots\ldots\ldots\ldots (2)$$

is the ratio of the total mobility of all phases, λ_T, upon the total system compressibility, c_T, which includes rock, fluid, and the apparent compressibility originating from steam condensation. Here p is pressure, x is distance from the injection plane, and t is time. Because the South Belridge diatomite is so finely layered and hydraulic-fracture length is generally greater than the height of a layer, a one-dimensional equation suffices.[9]

The position of the steam front, X_f, within each layer of the diatomite is obtained by performing a bulk-heat balance in the horizontal direction and assuming that layer properties are uniform and constant. After neglecting interlayer heat transfer we obtain

$$X_f = \int_0^t \frac{\dot{Q}_i}{M_T A_c \Delta T_i}, \quad \ldots\ldots\ldots\ldots\ldots\ldots\ldots\ldots\ldots\ldots\ldots\ldots\ldots (3)$$

where $\dot{Q}_i$ is the rate of heat injection, M_T is the total volumetric specific heat, A_c is the layer vertical cross-sectional area, and ΔT_i $(= T_i - T_o)$ is the saturated-steam temperature at the fracture face minus the initial layer temperature.

Over the portions of the formation not swept by steam-heat transport occurs by thermal conduction. Consistent with Eq. 1, one-dimensional heat conduction is described by

$$\frac{\partial^2 T}{\partial x^2} = \frac{1}{\alpha}\frac{\partial T}{\partial t};\ x > X_f, \quad \ldots\ldots\ldots\ldots\ldots\ldots\ldots\ldots\ldots\ldots\ldots\ldots\ldots (4)$$

where α $(= K/M_T)$ is the thermal diffusivity of the formation while K is the thermal conductivity.

History-Matching Procedure

Eqs. 1, 3, and 4 are used to interpret the response to steam injection during the Phase II pilot. A detailed description of the history-matching procedure is available elsewhere.[9] In summary, the diatomite interval at the pilot is subdivided into a series of isolated, one-dimensional layers by examining the porosity logs and the temperature responses in each observation well. Each isolated layer is then assigned the average properties calculated from the logs for all observation wells as a function of depth. Each layer is discretized in the horizontal, x, direction with the azimuth for all hydraulic fractures set to N21°E. Next, initial pressure and temperature are estimated for each layer according to the pressure decline caused by 10 years of primary production from 543N and the geothermal-temperature gradient. Boundary conditions are also assigned for each layer. To account for the flow resistance into a production fracture under compression, a 100-psia pressure at the fracture face is specified, even though the producers are pumped off. The inlet pressure is set to the downhole steam pressure, less a correction for capillary pressure.[9] The initial shape of the injection hydraulic fracture is inferred from the temperature-response data.

The pressure and temperature diffusion equations, Eqs. 1 and 3, are solved sequentially to simulate the invasion of steam and the flow of heat in unswept areas. Solution proceeds with a Galerkin finite-element technique and a Crank-Nicolson time-weighting scheme. Assumption of saturated steam conditions provides the requisite temperature profile in the steam zone. Eq. 3 is integrated numerically with the trapezoid rule to obtain the position of the steam front and the region over which each diffusion equation applies. At the fracture face, we use a finite-element interpolation to calculate the pressure gradient. Multiplication of pressure gradient by layer permeability, relative permeability of steam or water, cross-sectional area, and division by the viscosity of each phase yields the instantaneous injection rate.

Finally, the simulation parameters are adjusted until an acceptable match is obtained between field results and simulation. Initial temperature response is mainly caused by conduction; α for each layer is chosen to match the initial temperature response; and η for each layer is adjusted to match the total steam injection and deviations in the longer time temperature response from the results expected solely from heat conduction. The hydraulic-fracture length is increased as needed to match the temperature results at LO11, LO12, and MO2. We approximate growth of the steam-filled portion of the hydraulic fracture by increasing the cross-sectional area of a layer, subdividing the layer into old and new volumes, and assigning to the new volume initial temperatures and pressures as discussed above.

History Match

Steam injection is matched, as well as the temperature response in the outlying monitoring wells displayed in Fig. 2. Thus, the match is highly constrained. To achieve the match, α and M_T are fixed for each layer throughout the simulation, but hydraulic diffusivity and permeability are allowed to vary with time. Initially, the hydraulic diffusivities of layers on opposite sides of the injection fractures should be equal. After the first 220 days, they are allowed to vary independently.

For the best match of the response caused by steam injection in IN2U, M_T ranges between 66.0 and 72.5 Btu/ft^3-°F, α spans 0.11 to 0.42 ft^2/D, and η varies from lows of 0.11 ft^2/D to 8.1 ft^2/D. In the case of IN2L, M_T ranges between 68.6 and 71.6 Btu/ft^3-°F, α varies between 0.13 and 0.41 ft^2/D, while η ranges from 0.086 ft^2/D to a high of 1 ft^2/D. With typical parameters values and Eq. 2, we estimate that cycle permeabilities ranged from 0.010 to 0.70 md. The

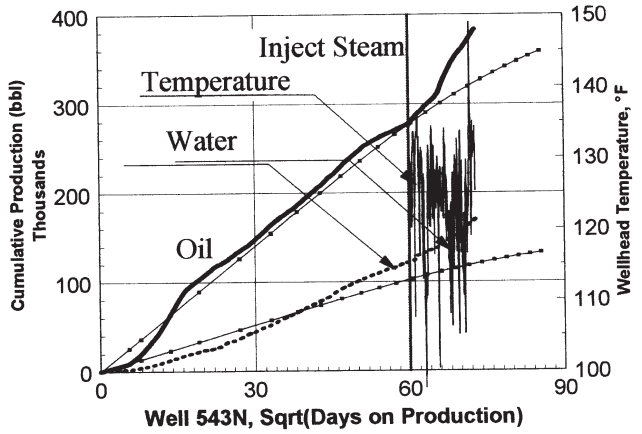

Fig. 5—Cumulative oil and water production in 543N.

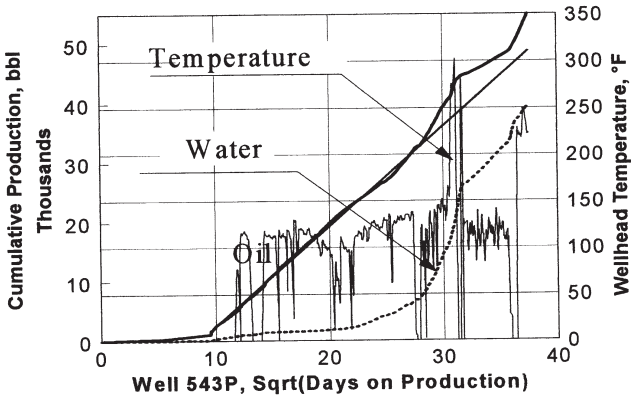

Fig. 6—Cumulative oil and water production in 543P.

variation in η and permeability is large because rock properties vary dramatically from layer to layer.

Figs. 3 and 4 contrast the actual (dashed line) and history match (solid line) cumulative steam injection in IN2U and IN2L, respectively. Overall, we find good agreement. The slopes of these curves are indicative of injectivity. In each figure, quite a large increase in slope occurs around 17 days$^{1/2}$ as a result of dramatic enlargement of fracture-injection area. Also indicated on Figs. 3 and 4 are the simulated amounts of steam that flowed into the western and eastern portions of the pilot volume. During steam injection through IN2U, it appears that a much greater portion of the injected steam flowed to the western portion of the pilot. While for IN2L, injection seems to be more balanced between the east and the west. Horizontal features of the upper portion of the formation, such as a network of fractures, allowed the western portion of the pilot opposite IN2U to accept much more steam. The location and the magnitude of such a feature will become apparent after the formation temperature response is reviewed.

Temperature logs from the observation wells reveal much about the distribution of injected steam, which cause heat, both vertically and areally. Full-interval temperature responses (700 to 2,000 ft) are given in **Figs. 7 and 8** from wells LO14 and LO15. These wells lie directly next to the injectors but on opposite sides. The horizontal dashed lines and the letters C through M denote the geologic layering of the pilot. Also, reported are history-match temperature responses. No simulated temperature response is reported in the interval from roughly 1,400 to 1,500 ft because the injection fractures are noncommunicating.

As with cumulative steam injection, the match is quite good. More importantly, temperature response is asymmetric to either side of the fracture and vertically. Toward the west, LO14 shows dramatic temperature response approaching 350°F between 960 and 1,120 ft, while LO15 shows at most a 100°F temperature increase across the same depths. The dramatic temperature response to the west of IN2U is inferred from the history match to be the result of steam entering a horizontal feature of relatively large permeability. Figs. 7 and 8 also show that temperature increase varies with depth. For instance, the M cycle at 1,820 ft has a considerable temperature response, but the L cycle at roughly 1,700 ft does not.

Although not displayed, temperature response in the observation wells located toward the outer edges of the injection-hydraulic fractures was equally asymmetric. Some geologic cycles heated preferentially, while others showed much less temperature response. In the

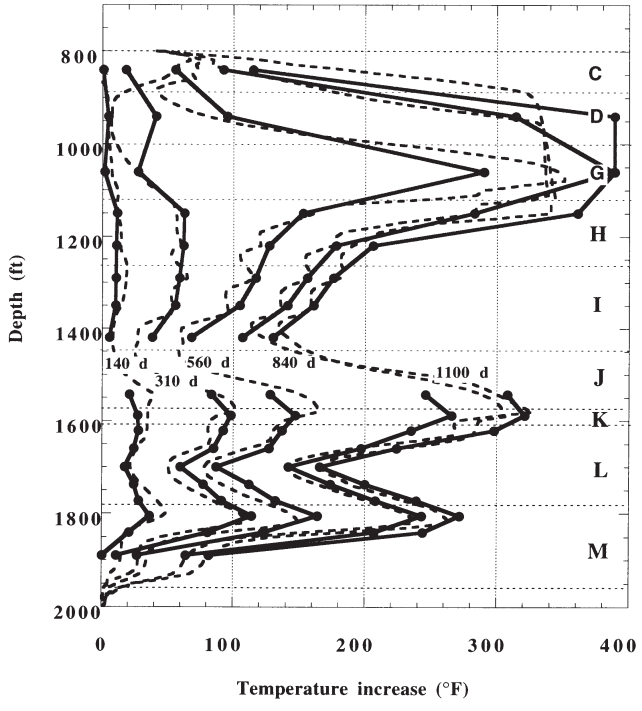

Fig. 7—Temperature response and history-match results for Well LO14.

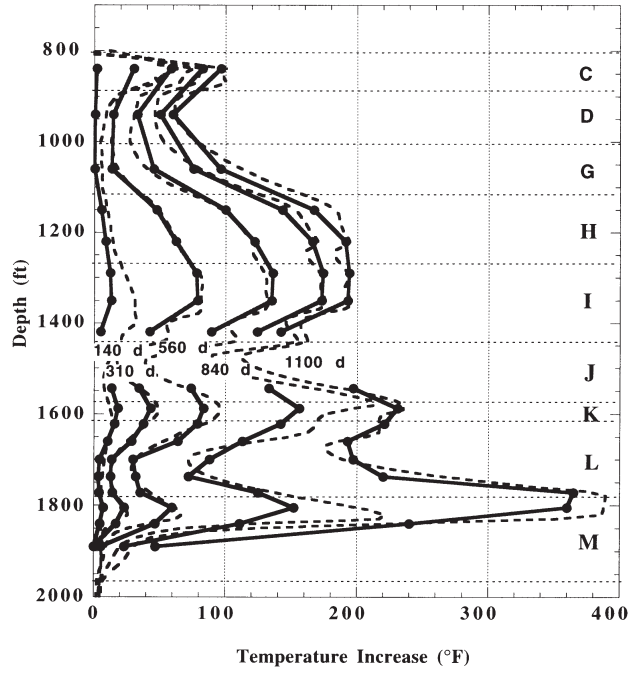

Fig. 8—Temperature response and history-match results for Well LO15.

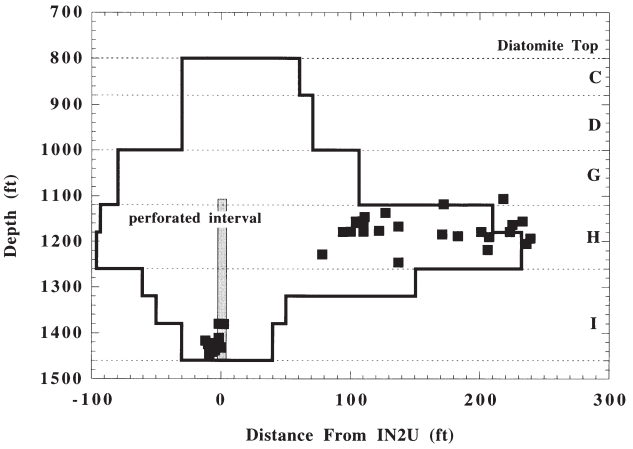

Fig. 9—Comparison between IN2U fracture shape from history matching and microseismic events.

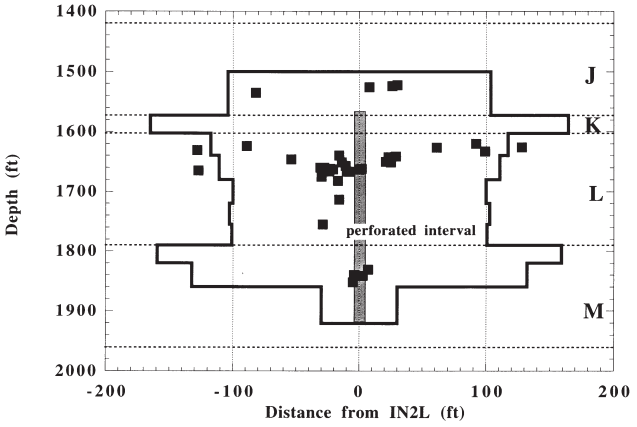

Fig. 10—Comparison between IN2L fracture shape from history matching and microseismic events.

case of heating opposite IN2U, wells located to the northeast generally showed temperature response before those to the south did.

Interestingly, the heat-communicating portion of the hydraulic fracture connected to IN2U assumed an asymmetric shape, while that of IN2L appeared to remain symmetric. **Figs. 9 and 10** detail the final shapes (after more than 1,000 days of steam injection) of the hydraulic fractures in IN2U and IN2L with a dark line. In each figure, the injection well is located at the origin and the darkly shaded rectangle gives the extent of the perforated zone. In the case of IN2U displayed in Fig. 9, the northern wing extends in excess of 220 ft, but the southern wing extends to only 100 ft. The asymmetric northern wing is necessary to simulate a temperature response at well MO1; however, a matching symmetric wing to the south would lead us to overpredict steam injection and temperature response substantially. These particular hydraulic-fracture shapes and companion hydraulic diffusivities for each layer have allowed us to match cumulative steam injection and the volumetric heating indicated by temperature logs. Thus, the match is highly constrained and honors all available data.

Figs. 9 and 10 also present results from microseismic monitoring of the hydraulic fracturing process as dark squares[1]. The squares represent the locations of microseismic events found while analyzing the arrival times of shear waves at the observation wells.

In general, the extent of the hydraulic fractures interpreted from the temperature data appears somewhat greater than that from the microseismic analysis. In both cases, there is little reason to believe that a fracture undergoing continuous steaming near the fracture gradient would not increase its area beyond that created during the initial hydraulic-fracturing process. However, the microseismic event locations are consistent with the shape of each fracture. Moreover in the case of IN2U, the microseismic event locations are diagnostic of hydraulic-fracture asymmetry. In fact, we conclude that microseismic activity during fracturing is diagnostic of the most active portions of a hydraulic fracture, because independent analyses have yielded similar fracture shapes and orientations for the Phase II pilot. Further, we find that regions of the formation where multiple microseismic events were recorded generally accepted steam much more readily than regions of little microseismic activity.

Conclusions

The Phase II steamdrive pilot in the South Belridge diatomite demonstrated that steam could be injected across the entire diatomite interval, that significant heating of the formation occurs as a result of steam injection, and that significant incremental oil is produced. With a simple model incorporating the first-order physics of steamdrive in diatomite we have been able to interpret pilot results. The pilot showed significant heating as a result of steam and hot-condensate convection as opposed to heating of the formation only by simple conduction. Substantial increases in injection that occurred over time were linked to growth in the size of the injection-hydraulic fracture and increases in formation permeability.

Heating of the formation, although significant, was asymmetrical. Regions of the formation with relatively large permeability accepted the largest amount of steam and demonstrated the greatest amount of heating. Fracture shape also contributed to the pattern of heating. In comparing pilot-heating results with a microseismic analysis of fracture shape, it is found that regions of high microseismic activity during the hydraulic-fracturing process generally correspond to areas of most active steam injection. Also, the general shape of hydraulic fractures indicated by microseismic analysis appears to correspond to that inferred from the distribution of temperature within the formation.

Acknowledgments

We thank CalResources LLC for releasing the injection, pressure, and temperature log data from the Phase II pilot. This work was supported by the Assistant Secretary for Fossil Energy, Office of Gas and Petroleum Technology, under contract No. DE-ACO3-76FS00098 to the Lawrence Berkeley Laboratory of the U. of California.

Nomenclature

A_c = cross-sectional area, L^2, ft^2
c_T = total compressibility, Lt^2/m, psi^{-1}
K = thermal conductivity, m/t^3T, Btu/D-ft-°F
M_T = volumetric specific heat, m/Lt^2T, Btu-ft^3-°F
p = pressure, m/Lt^2, psi
$\dot{Q}_i$ = heat injection rate, m/Ls^2, Btu/ft^3-D
t = time, t, D
T = temperature, T, °F
T_i = steam injection temperature, T, °F
x = distance, L, ft
X_f = steam front position, L, ft
α = thermal diffusivity, L^2/t, ft^2/D
η = hydraulic diffusivity, L^2/t, ft^2/D
λ_T = total mobility, L^3t/m, ft^2/psi-D

References

1. Ilderton, D.C. *et al.*: "Passive Imaging of Hydrofractures in the South Belridge Diatomite," *SPEFE* (March 1996) 46.
2. Patzek, T.W.: "Surveillance of the South Belridge Diatomite," paper 24040 presented at the 1992 SPE Western Regional Meeting, Bakersfield, California, 30 March–1 April.
3. Nikravesh, M. *et al.*: "Neural Networks for Field-Wise Waterflood Management in Low Permeability, Fractured Oil Reservoirs," paper 35721, presented at the 1996 SPE Western Regional Meeting, Anchorage, 22–24 May.

4. Kumar, M. and Beatty, F.D.: "Cyclic Steaming in Heavy Oil Diatomite," paper 29623, presented at the 1995 SPE Western Regional Meeting, Bakersfield, California, 8–10 March.
5. Johnston, R.M. and Shahin, G.T.: "Interpretation of steamdrive Pilots in the Belridge Diatomite," paper 29621, presented at the 1995 SPE Western Regional Meeting, Bakersfield, California, 8–10 March.
6. Schwartz, D.E.: "Characterizing the Lithology, Petrophysical Properties, and Depositional Setting of the Belridge Diatomite, South Belridge Field, Kern County, California," *Studies of the Geology of the San Joaquin Basin*, S.A. Graham and H.C. Olson (eds.), The Pacific Section Society of Economic Paleontologists and Mineralogists, Los Angeles, California, (1988) 281–301.
7. Vinegar, H.J. *et al.*: "Active and Passive Seismic Imaging of a Hydraulic Fracture in Diatomite," *JPT* (January 1992) 28, 88.
8. Kovscek, A.R., Johnston, R.M., and Patzek, T.W.: "Interpretation of Hydrofracture Geometry During Steam Injection Using Temperature Transients II. Asymmetric Hydrofractures," *In Situ* **20**, (1996) 289–309.
9. Kovscek, A.R., Johnston, R.M., and Patzek, T.W.: "Interpretation of Hydrofracture Geometry During Steam Injection Using Temperature Transients I. Model Formulation and Verification," *In Situ* **20,** (1996) 251–288.
10. Marx, J.W., and Langenheim, R.H.: "Reservoir Heating by Hot Fluid Injection," *Trans.,* AIME **216**, (1959) 312–315.

SI Metric Conversion Factors

acre	$\times 4.046\,873$	$E-01$	$= \text{ha}$
bbl	$\times 1.589\,873$	$E-01$	$= \text{m}^3$
Btu	$\times 1.055\,056$	$E+00$	$= \text{kJ}$
ft	$\times 3.048^*$	$E-01$	$= \text{m}$
ft^2	$\times 9.290\,304^*$	$E-02$	$= \text{m}^2$
°F	$(°\text{F}-32)/1.8$		$= °\text{C}$

*Conversion factor is exact.

SPEPF

Tony Kovscek is an assistant professor of petroleum engineering at Stanford U. His interests include fluid and heat flow in tight-fractured rocks and foams for mobility control of gas-injection processes. Before joining Stanford, he worked in the Earth Sciences Div. of Lawrence Berkeley Natl. Laboratory. He holds a PhD degree from the U. of California, Berkeley, and a BS degree from the U. of Washington. Both degrees are in chemical engineering. Photo unavailable. **Mike Johnston** works for CalResources LLC in Bakersfield, California. He has worked in various engineering capacities on many California oil fields since 1984. He holds BS and MS degrees in geological engineering from the U. of Missouri, Rolla. Photo unavailable. **Tad Patzek** is an associate professor of petroleum engineering at the U. of California, Berkeley. Previously, he worked for Shell Western E&P and in the Enhanced Recovery Research Dept. of Shell Development. His research activities include 3D modeling of foam flow in porous media with the population balance method; diffusion stability of stationary foams in porous media; the development of a finite-difference simulator of multicomponent, multiphase, nonisothermal flow in porous media; the use of steam to clean hydrocarbon spills; microearthquake imaging of massive hydrofractures; neural-network models of fluid injection and withdrawal in tight rock; and inverse modeling of steam injection into diatomite. He holds a PhD degree in chemical engineering from Silesian Technical U., Poland.

Patzek